Radiative decays of excited vector mesons

F. E. Close
Department of Theoretical Physics, University of Oxford, Keble Road, Oxford, OX1 3NP, England

A. Donnachie
Department of Physics and Astronomy, University of Manchester, Manchester M13 9PL, England

Yu. S. Kalashnikova
ITEP, Moscow, Russia

(Received 16 January 2002; published 23 April 2002)

Radiative decays of the 1^3S_1 radial and 1^3D_1 orbital excitations of the ρ, ω, and ϕ are calculated in the quark model, using wave functions obtained variationally from the Hamiltonian with standard quark-model parameters. The larger radiative widths should be measurable at new high-intensity facilities being proposed, and in some cases may be measurable in data from existing experiments. The radiative decays are a strong discriminator between the 1^3S_1 and 1^3D_1 excitations, and can also be used to provide unique information about the decay products.

DOI: 10.1103/PhysRevD.65.092003 PACS number(s): 13.20.Jf

I. INTRODUCTION

Radiative decays offer a rather direct probe of hadron structure. The coupling to the charges and spins of constituents reveals detailed information about wave functions and can discriminate among models. This can be particularly relevant in distinguishing gluonic excitations of the π,ρ (hybrids) from conventional excitations with these overall J^{PC}. For example, in a hybrid 1^{--} the $q\bar{q}$ are in a spin singlet, while for the 0^{-+} they are in a triplet; in each case this is the reverse of what one is used to.

In this paper we investigate potential tests using radiative decays of vector mesons to separate $q\bar{q}$ states from hybrids in the 1–2 GeV mass region, where light-flavor states are predicted to occur, and where *prima facie* candidates have been identified. Exotic $J^{PC}=1^{-+}$ signals have been reported around 1.4–1.6 GeV mass; the systematics of 1^{--} states in this region seem to point toward gluonic excitations being present and there are tantalizing hints of unusual activity in the 0^{-+} partial wave in the 1.6–1.8 GeV region.

A quite separate problem is posed by the scalar mesons. It seems likely that the $a_0(980)$ and $f_0(980)$ are intimately linked to the $K\bar{K}$ threshold with significant $q^2\bar{q}^2$ affinity. Then the $q\bar{q}$ mesons are manifested in the 1.3–1.7 GeV region, presumably mixed with the 0^{++} glueball of the lattice. A direct measure of their flavor content would resolve this issue. We suggest that radiative transitions from the $2S$ and $1D$ vector excitations can answer this.

The forthcoming generation of e^+e^- facilities, such as the upgrade of VEPP at Novosibirsk, the use of initial state radiation at BABAR to study light-quark vectors and the proposed dedicated e^+e^- collider PEP-N, promise more than two orders of magnitude increase in data over present machines. There is a complementary high-intensity program of photo- and electroproduction at Jefferson Laboratory. Together these will enable data on radiative decays to be obtained comparable in quality to those of present hadronic channels. Thus it is timely to ask whether, and under what circumstances, these data will be able to make sensitive probes of radiative transitions and to isolate evidence for gluonic degrees of freedom. Radiative decays offer an alternative approach to resolving the various problems we have outlined. They are a much better probe of wave functions, and hence of models, than are hadronic decays. They can access final states which are kinematically excluded for hadronic decays. Historically, studies of light-quark radiative transitions have been restricted to the ground states. We extend these calculations to decays from the $2S$ and $1D$ excitations of the ρ, ω, and ϕ to $1S$, $2S$, and $1P$ states, as these processes are now becoming accessible to experiment. Our results are encouraging. We find that certain channels, with large partial widths, allow a clean separation of the $2S$ and $1D$ $q\bar{q}$ states, for example, $f_2(1270)\gamma$ for the $\rho(1450)$, $f_1\gamma$ for the $\rho(1700)$, $f_2'(1525)\gamma$ for the $\phi(1690)$, and $f_1(1420)$ for the $\phi(1900)$. Additionally, the radiative decays of the $\rho(1700)$ and $\phi(1900)$ to $n\bar{n}$ and $s\bar{s}$ scalars, respectively, probe the f_0 sector and provide a potential entrée to flavor filtering.

In Sec. II we review the present status of the interesting mesons in the 1–2 GeV mass range. We then turn in Secs. III and IV to establishing our formalism for calculating radiative transition rates. Their magnitudes are computed in Sec. V, and in Sec. VI we identify a strategy for exploiting these results in forthcoming experiments.

II. MESONS IN THE 1–2 GeV MASS RANGE

The existence of two higher isovector-vector mesons, the $\rho(1450)$ and the $\rho(1700)$, their isoscalar counterparts, the $\omega(1420)$ and $\omega(1650)$, and an associated hidden-strangeness state, the $\phi(1680)$, is well established [1]. Although there is general consensus on the existence of these states, there is considerable disparity on their masses and widths. Further, what is known about the composition of their hadronic decays raises fundamental questions about the nature of these

states and our understanding of the mechanism of hadronic decays.

An apparently natural explanation for the higher-mass vector states is that they are the first radial 2^3S_1 and first orbital 1^3D_1 excitations of the ρ and ω and the first radial excitation of the ϕ, as the generally accepted masses [1] are close to those predicted by the quark model [2]. However, this argument is suspect as the masses of the corresponding $J^P=1^-$ strange mesons are less than the predictions, particularly for the 2^3S_1 at 1414 ± 15 MeV [1] compared to the predicted 1580 MeV [2]. Quite apart from comparing predicted and observed masses, one would expect the $n\bar{n}$ mesons to be 100–150 MeV lighter than their strange counterparts, putting the 2^3S_1 at less than 1300 MeV and the 1^3D_1 below 1600 MeV. Also this interpretation faces a further problem. The data on the 4π channels in e^+e^- annihilation and τ decay are not compatible with the $^3P_0$ model [3–6], which works well for decays of established ground-state mesons. For example, widths predicted to be large are found to be so; widths predicted to be small, are found to be so; calculated widths agree with data to within 25–40 %; and signs of amplitudes are predicted correctly. As far as one can ascertain the $^3P_0$ model is reliable, but it has not been seriously tested for the decays of excited states.

The $^3P_0$ model predicts that the decay of the isovector 2^3S_1 to 4π is extremely small: $\Gamma_{2S\to a_1\pi}\sim3$ MeV and $\Gamma_{2S\to h_1\pi}\sim1$ MeV, and other possible 4π decays are even smaller. For the isovector 1^3D_1 the model predicts that the $a_1\pi$ and $h_1\pi$ decays are large and equal: $\Gamma_{1D\to a_1\pi}\sim\Gamma_{1D\to h_1\pi}\sim105$ MeV. All other possible 4π channels are small. As $h_1\pi$ contributes only to the $\pi^+\pi^-\pi^0\pi^0$ channel in e^+e^- annihilation, and $a_1\pi$ contributes to both $\pi^+\pi^-\pi^+\pi^-$ and $\pi^+\pi^-\pi^0\pi^0$, then after subtraction of the $\omega\pi$ cross section from the total $\pi^+\pi^-\pi^0\pi^0$, one expects that $\sigma(e^+e^-\to\pi^+\pi^-\pi^0\pi^0)>\sigma(e^+e^-\to\pi^+\pi^-\pi^+\pi^-)$. This contradicts observation [7] over most of the available energy range, in which $\sigma(\pi^+\pi^-\pi^+\pi^-)\approx2\sigma(\pi^+\pi^-\pi^0\pi^0)$. Further, and more seriously, it has been shown recently by the CMD Collaboration at Novosibirsk [7] and by CLEO [8] that the dominant channel by far in 4π (excluding $\omega\pi$) up to $\sim$1.6 GeV is $a_1\pi$. This is quite inexplicable in terms of the $^3P_0$ model. So the standard picture is wrong for the isovectors, and there are serious inconsistencies in the isoscalar channels as well. One possibility is that the $^3P_0$ model is simply failing when applied to excited states, which is an intriguing question in itself. An alternative is that there is new physics involved.

A favored hypothesis is to include vector hybrids [9–11], that is, $q\bar{q}g$ states. The reason for this is that, first, hybrid states occur naturally in QCD, and, secondly, that in the relevant mass range the dominant hadronic decay of the isovector vector hybrid ρ_H is believed to be $a_1\pi$ [10]. The masses of light-quark hybrids have been obtained in lattice-QCD calculations [12–16], although with quite large errors. Results from lattice QCD and other approaches, such as the bag model [17,18], flux-tube models [19], constituent gluon models [20], and QCD sum rules [21,22], show considerable variation from each other. So the absolute mass scale is somewhat imprecise, predictions for the lightest hybrid lying between 1.3 and 1.9 GeV. However, most models and lattice gauge calculations predict the lightest hybrids to be at the upper end of this mass range. It does seem generally agreed that the mass ordering is $0^{-+}<1^{-+}<1^{--}<2^{-+}$.

Evidence for the excitation of gluonic degrees of freedom has emerged in several processes. A clear exotic $J^{PC}=1^{-+}$ resonance, the $\pi_1(1600)$, is seen [23] in the $\eta'(958)\pi$ channel in the reaction $\pi^-N\to(\eta'(958))\pi N$. Two experiments [24,25] have evidence for this exotic in the $\rho^0\pi^-$ channel in the reaction $\pi^-N\to(\pi^+\pi^-\pi^-)N$. A peak in the $\eta\pi$ mass spectrum at $\sim$1400 MeV with $J^{PC}=1^{-+}$ in $\pi^-N\to(\eta\pi^-)N$ has also been interpreted as a resonance [26]. Supporting evidence for the 1400 MeV state in the same mode comes from $\bar{p}p\to\eta\pi^-\pi^+$ [27]. There is evidence [28] for two isovector 0^{-+} states in the mass region 1.4–1.9 GeV, $\pi(1600)$ and $\pi(1800)$. The quark model predicts only one. Taking the mass of the $1^{-+}\sim1.4$ GeV and assuming the generally agreed mass ordering, then the 0^{-+} is at $\sim$1.3 GeV and the lightest 1^{--} at $\sim$1.65 GeV, which is in the range required for the mixing hypothesis to work. However, if the $\pi_1(1600)$ is the lightest 1^{-+} state, so that the vector hybrids are comparatively heavy, say $\sim$2.0 GeV, then strong mixing with the radial and orbital excitations would be less likely. At this stage we should keep an open mind and consider both options.

The scalar mesons in the mass range 1.3–1.7 GeV provide another place in which to look for gluonic hadrons as lattice calculations have now become sufficiently stable to predict [29], in the quenched approximation, that the lightest glueball has $J^{PC}=0^{++}$ and is in the mass range 1.45–1.75 GeV.

There are more scalar mesons than the simple $q\bar{q}$ 1^3P_0 nonet can accommodate. The $f_0(980)$ and $a_0(980)$ mesons most probably do not belong to this nonet [30,31], and are either $q^2\bar{q}^2$ states or $K\bar{K}$ molecules. In any case they are associated with the nearby $K\bar{K}$ threshold. Then the possible candidates for the $q\bar{q}$ 1^3P_0 nonet are $a_0(1450)$, $K_0^*(1430)$, $f_0(1370)$, $f_0(1500)$, and $f_0(1710)$. There is an obvious excess in the isoscalar-scalar sector, with the natural inference of there being a glueball state present.

The lightest scalar glueball should mix with the $q\bar{q}$ scalars in the same mass region and recent studies [32] on a coarse-grained lattice suggest that such mixing is significant. While analyses [30,33–35] of the mixing differ in some details, the conclusions exhibit common robust features. The flavor content is predicted to have $n\bar{n}$ and $s\bar{s}$ in phase for the $f_0(1370)$ and $f_0(1710)$ [SU(3)-singlet tendency], out of phase for the $f_0(1500)$ [SU(3)-octet tendency], and to have a glueball component in all three states. The detailed pattern of mixing was determined in [35] by studying the complete set of decay branching ratios into pseudoscalars [36] for the $f_0(1370)$, $f_0(1500)$, and $f_0(1710)$, and confirmed by comparing relative production rates. The preferred scenario [35] gives the bare masses as $m_g=1443\pm24$ MeV, $m_{n\bar{n}}=1377\pm10$ MeV, and $m_{s\bar{s}}=1674\pm10$ MeV. Other solutions have been found which have either a heavy glueball, $m_g>m_{s\bar{s}}$, or a light glueball, $m_g<m_{n\bar{n}}$, and although less consistent with

the data they cannot be ruled out completely. The preferred solution is consistent with what one would expect naively from the $s\bar{s}$-$n\bar{n}$ mass difference of about 300 MeV, and places the glueball at the lower end of the mass range given by the lattice calculations.

The mixing scheme implies that the isovector partner of the $n\bar{n}$ state, the a_0, should have a mass of about 1400 MeV. There is an indication that this state has been observed [37]. Any confirmation of this controversial $a_0(1450)$ is of paramount importance, not only for the problem of glueball-quarkonia mixing, but for the nature of the 0^{++} mesons.

The emerging data suggest that gluonic excitations, for both hybrids and glueballs, are rather lighter than quenched-lattice predictions and that their effects will be apparent in the 1–2 GeV mass range. As we shall see, radiative transitions can shed new light on the matter.

III. RADIATIVE DECAYS OF QUARKONIA

The initial meson A, with mass m_A, decays at rest to the final-state meson B, with mass m_B and a photon with three-momentum $\mathbf{p}$. In the nonrelativistic quark model the standard expression for the transition amplitude has the form

$$\mathbf{M}_{A\to B}=\mathbf{M}^{q}_{A\to B}+\mathbf{M}^{\bar{q}}_{A\to B}, \tag{1}$$

where $\mathbf{M}^{q}_{A\to B}$ and $\mathbf{M}^{\bar{q}}_{A\to B}$ describe the emission of the photon from the quark and antiquark, respectively:

$$\mathbf{M}^{q}_{A\to B} = \frac{I_q}{2m_q}\int d^3k[\mathrm{Tr}\{\phi_B^\dagger(k-\tfrac{1}{2}p)\phi_A(k)\}(2\mathbf{k}-\mathbf{p}) - i\,\mathrm{Tr}\{\phi_B^\dagger(\mathbf{k}-\tfrac{1}{2}\mathbf{p})\sigma\phi_A(\mathbf{k})\}\times\mathbf{p}] \tag{2}$$

and

$$\mathbf{M}^{\bar{q}}_{A\to B} = \frac{I_{\bar{q}}}{2m_q}\int d^3k[\mathrm{Tr}\{\phi_A(\mathbf{k})\phi_B^\dagger(\mathbf{k}+\tfrac{1}{2}\mathbf{p})\}(2\mathbf{k}+\mathbf{p}) - i\,\mathrm{Tr}\{\phi_A(\mathbf{k})\sigma\phi_B^\dagger(\mathbf{k}+\tfrac{1}{2}\mathbf{p})\}\times\mathbf{p}], \tag{3}$$

where I_q and $I_{\bar{q}}$ are isospin factors and m_q is the quark mass.

We use matrix forms for the wave functions. For a meson M, with quark spin 0, total angular momentum j, and magnetic quantum number m the wave function is given by

$$\phi_M(\mathbf{q})=\frac{1}{\sqrt{2}}\hat{\mathbf{1}}Y_{jm}(\hat{q})R_M(q). \tag{4}$$

For a meson with total angular momentum j, quark spin 1, and quark orbital momentum l, the corresponding wave function is

$$\phi_M(\mathbf{q})=\frac{1}{\sqrt{2}}\mathbf{Y}_{jlm}(\hat{q})\sigma R_M(q). \tag{5}$$

Here $\hat{\mathbf{1}}$ is the 2×2 unit matrix and σ is the Pauli matrix. The $R_M(q)$ are the mesonic radial wave functions in the momentum representation

We calculate in the center of mass of e^+e^- annihilation as in that case the virtual photon is polarized, and one can study angular distributions with respect to the beam direction. These are given in Appendix A. In Appendix B we show how to derive the helicity amplitudes and their relation to the formalism used in the paper, which enables the results to be transferred to any frame of reference.

The differential decay rate is evaluated for initial photon polarization $m_0=1$ and is given by

$$\frac{d\Gamma}{d\cos\theta}=4p\frac{E_B}{m_A}\alpha I\sum|M_{A\to B}|^2 \tag{6}$$

where the sum is over final-state polarizations. In Eq. (6) E_B is the center-of-mass energy of the final meson and $I=I_q^2=I_{\bar{q}}^2$ is the isospin factor. We consider the radiative decays of neutral vector mesons, so the isospin factors for decays between $n\bar{n}$ or $s\bar{s}$ states are

$$I=\begin{cases}\frac{1}{36} & \text{for } n\bar{n}\to n\bar{n} \text{ with same isospin,}\\ \frac{1}{4} & \text{for } n\bar{n}\to n\bar{n} \text{ with different isospin,}\\ \frac{1}{9} & \text{for } s\bar{s}\to s\bar{s}.\end{cases} \tag{7}$$

We take $\eta=\eta_8=(u\bar{u}+d\bar{d}-2s\bar{s})/\sqrt{6}$ and $\eta'=\eta_1=(u\bar{u}+d\bar{d}+s\bar{s})/\sqrt{3}$ so the isospin factors for decays to η and η' are

$$I=\begin{cases}\frac{1}{108} & \text{for } n\bar{n} \text{ with isospin } 0\to\eta,\\ \frac{1}{12} & \text{for } n\bar{n} \text{ with isospin } 1\to\eta,\\ \frac{1}{54} & \text{for } \bar{n} \text{ with isospin } 0\to\eta'\\ \frac{1}{6} & \text{for } n\bar{n} \text{ with isospin } 1\to\eta',\\ \frac{2}{27} & \text{for } s\bar{s}\to\eta,\\ \frac{1}{27} & \text{for } s\bar{s}\to\eta'.\end{cases} \tag{8}$$

Radial wave functions are found variationally from the Hamiltonian

$$H=\frac{p^2}{m_q}+\sigma\tau-\frac{4}{3}\frac{\alpha_s}{r}+C \tag{9}$$

with standard quark-model parameters $m_q=0.33$ GeV for u and d quarks, $m_q=0.45$ GeV for s quarks, $\sigma=0.18$ GeV^2, and $\alpha_s=0.5$. The wave functions are taken to be Gaussian, that is, of the form $\exp[-k^2/(2\beta_M^2)]$ multiplied by the appropriate polynomials, and β treated as the variational parameter in Eq. (9) for each of the $1S$, $1P$, $2S$, and $1D$ states. The resulting values of β and the corresponding masses for $n\bar{n}$ states are given in Table I, and those for $s\bar{s}$ states in Table II.

It is well-known that the use of exact wave functions is necessary to reproduce the low-energy theorems. For example, the expression for the $E1$ transition amplitude [Eqs.

TABLE I. Effective masses and corresponding β from the variational solution of Eq. (9) for $n\bar{n}$ states.

	M (GeV)	β (GeV)
$1S$	0.700	0.313
$1P$	1.262	0.274
$2S$	1.563	0.253
$1D$	1.703	0.255

(2) and (3) in the $p=0$ limit] can be written in the dipole form using the relation $\vec{k}=im_q[H\vec{r}]/2$. The amplitude is proportional to the overlap integral

$$\frac{im_q}{2}(E_A-E_B)\int r^3dr\,\psi_A(r)\psi_B(r), \tag{10}$$

which immediately gives the threshold p^3 behavior of the electromagnetic width demanded by gauge invariance. This means that not only should the ''correct'' values of the oscillator parameter β be used, but also the masses of the initial and final states should be taken to be ''correct'' eigenvalues of the quark model Hamiltonian (9). One can systematically improve the variational ansatz adopted for the wave functions, using more sophisticated trial wave functions [2,38] or numerical solutions [38]. Fortunately, in most cases in practice, the ''correct'' masses and the known physical masses do not differ by much, and the resulting differences in the decay widths are smaller than other uncertainties in the calculation. However this is not true of decays to the pseudoscalars π, η, and η'.

The constituent quark model in its naive form (9) works reasonably well, with the exception of the lowest pseudoscalars as the Goldstone-boson nature of these particles is not naturally accommodated. More complicated versions, such as [2], include relativistic kinematics and properly smeared spin-dependent terms, and the agreement with data on spectra is quite remarkable. Similar results are obtained in the QCD string model [39], where it is shown that the constituent masses of quarks appear dynamically due to the QCD-inspired string-type interaction. The most serious drawback of such a picture is that the issue of chiral symmetry breaking is completely beyond its scope. It is possible to describe the low-lying pion in the constituent quark models, but the Goldstone nature of the pion is completely lost. However, the chiral properties can be naturally incorporated into the constituent picture in the framework of the Hamiltonian approach in the Coulomb gauge [40]. In this approach, a chirally noninvariant vacuum is constructed, which implies the existence of the Goldstone boson as the lowest $q\bar{q}$ state. The axial current is conserved in the chiral limit, and all the relations of current algebra are satisfied. Some results of this approach are relevant to our purposes. First, even in the chiral limit, where the pionic wave function has very peculiar properties, the other mesons behave to large extent as quark model ones (for the details, see [41]). Second, while the confining interaction alone can describe the observed π-ρ splitting, the predictions for the quark condensate and pion decay constant are too small, and can be improved by inclusion of the hyperfine interaction [42]. The net result of these studies is that if the effective degrees of freedom are properly defined, then the constituent quark model is a good approximation, with most important ingredients absorbed in the quark-model parameters.

TABLE II. Effective masses and corresponding β from the variational solution of Eq. (9) for $s\bar{s}$ states.

	M (GeV)	β (GeV)
$1S$	1.000	0.355
$1P$	1.527	0.307
$2S$	1.793	0.285
$1D$	1.932	0.285

This means that, as a first approximation, the mesonic wave functions can be found from the Hamiltonian (9). Also, for the pion, the ''correct'' β should be larger than the 313 MeV for the $1S$ states shown in Table I. We will return to this point below.

IV. RADIATIVE DECAY WIDTHS OF VECTOR MESONS

Expressions for the full angular distributions for the radiative decay widths of the 1^3S_1, 2^3S_1, and 1^3D_1 neutral vector mesons are given in Appendix A. Here we give only the total widths. In these results we define

$$\beta^2=\frac{2\beta_A^2\beta_B^2}{(\beta_A^2+\beta_B^2)} \tag{11}$$

and

$$\lambda=\frac{\beta_A^2}{2(\beta_A^2+\beta_B^2)}. \tag{12}$$

A method for deriving the following expressions when $\beta_A=\beta_B$ is given in Appendix B. The generalization to arbitrary β_A and β_B is straightforward but algebraically tedious:

$1^3S_1\to1^1S_0$

$$\Gamma_S^0=\frac{4}{3}\alpha p\frac{E_B}{m_A}\frac{p^2}{m_q^2}IF_{S1}^2. \tag{13}$$

$2^3S_1\to1^1S_0$

$$\Gamma=\frac{3}{2}\left[\left(\frac{\beta^2}{\beta_A^2}-1\right)+\frac{2\lambda^2p^2}{3\beta_A^2}\right]^2\Gamma_S^0. \tag{14}$$

$2^3S_1\to2^1S_0$

$$\Gamma=\frac{9}{4}\left[\left(\frac{5\beta^4}{3\beta_A^2\beta_B^2}-1\right)+\frac{4\lambda^2p^2}{3\beta^2}\left(\frac{\beta^4}{3\beta_A^2\beta_B^2}-1\right)+\frac{4\lambda^2p^4}{9\beta_A^2\beta_B^2}\right]^2\Gamma_S^0. \tag{15}$$

In Eqs. (13), (14), and (15) F_{S1} is defined by

$$F_{S1}=\frac{\beta^3}{\beta_A^{3/2}\beta_B^{3/2}}\exp\left(-\frac{p^2}{8(\beta_A^2+\beta_B^2)}\right). \tag{16}$$

$2^3S_1\to 1^3P_0$

$$\Gamma=\frac{16}{27}\alpha p\frac{E_B}{m_A}\frac{\beta^2}{m_q^2}\left[G_E^2-\frac{p^2}{2\beta^2}G_EG_M+\frac{1}{16}\left(\frac{p^2}{\beta^2}\right)^2G_M^2\right]IF_{S2}^2, \tag{17}$$

$2^3S_1\to 1^3P_1$

$$\Gamma=\frac{16}{9}\alpha p\frac{E_B}{m_A}\frac{\beta^2}{m_q^2}\left[G_E^2+\frac{p^2}{4\beta^2}G_EG_M+\frac{1}{32}\left(\frac{p^2}{\beta^2}\right)^2G_M^2\right]IF_{S2}^2. \tag{18}$$

$2^3S_1\to 1^3P_2$

$$\Gamma=\frac{80}{27}\alpha p\frac{E_B}{m_A}\frac{\beta^2}{m_q^2}\left[G_E^2+\frac{p^2}{4\beta^2}G_EG_M+\frac{7}{160}\left(\frac{p^2}{\beta^2}\right)^2G_M^2\right]IF_{S2}^2. \tag{19}$$

In Eqs. (17), (18), and (19) F_{S2} is defined by

$$F_{S2}=\frac{\beta^4}{\beta_A^{3/2}\beta_B^{5/2}}\exp\left(-\frac{p^2}{8(\beta_A^2+\beta_B^2)}\right), \tag{20}$$

G_E by

$$G_E=\frac{5\beta^2}{2\beta_A^2}-\frac{3}{2}+\frac{\lambda^2p^2}{\beta_A^2}, \tag{21}$$

and G_M by

$$G_M=\frac{4\lambda\beta^2}{\beta_A^2}+\left(\frac{\beta^2}{\beta_A^2}-1\right)(6\lambda-3)+\frac{2\lambda^2p^2}{\beta_A^2}(2\lambda-1). \tag{22}$$

$1^3D_1\to 1^1S_0$

$$\Gamma_D^0=\frac{8}{45}\alpha p\frac{E_B}{m_A}\lambda^4\frac{p^4}{\beta^4}\frac{p^2}{m_q^2}IF_{D1}^2. \tag{23}$$

$1^3D_1\to 2^1S_0$

$$\Gamma=\frac{3}{2}\left[\left(\frac{2\lambda^2p^2}{3\beta_B^2}-1\right)+\frac{7\beta^2}{3\beta_B^2}\right]^2\Gamma_D^0. \tag{24}$$

In Eqs. (23) and (24) F_{D1} is defined by

$$F_{D1}=\frac{\beta^5}{\beta_A^{7/2}\beta_B^{3/2}}\exp\left(-\frac{p^2}{8(\beta_A^2+\beta_B^2)}\right). \tag{25}$$

$1^3D_1\to 1^3P_0$

$$\Gamma=\frac{80}{27}\alpha p\frac{E_B}{m_A}\frac{\beta^2}{m_q^2}\left(1+\frac{p^2}{5\beta^2}\lambda(1+2\lambda)+\frac{p^4}{10\beta^4}\lambda^2(-1+2\lambda)\right)^2IF_{D2}^2. \tag{26}$$

$1^3D_1\to 1^3P_1$

$$\Gamma=\frac{20}{9}\alpha p\frac{E_B}{m_A}\frac{\beta^2}{m_q^2}\left(1+\frac{p^2}{5\beta^2}\lambda(7+4\lambda)+\frac{p^4}{50\beta^4}\lambda^2(5+68\lambda+8\lambda^2)+\frac{4p^6}{25\beta^6}\lambda^3(-2+3\lambda+2\lambda^2)+\frac{2p^8}{25\beta^8}\lambda^4(1-4\lambda+4\lambda^2)\right)IF_{D2}^2, \tag{27}$$

$1^3D_1\to 1^3P_2$

$$\Gamma=\frac{4}{27}\alpha p\frac{E_B}{m_A}\frac{\beta^2}{m_q^2}\left(1+\frac{p^2}{5\beta^2}\lambda(17+4\lambda)+\frac{p^4}{10\beta^4}\lambda^2(83-316\lambda+520\lambda^2)+\frac{22p^6}{5\beta^6}\lambda^3(1-6\lambda+8\lambda^2)+\frac{8p^8}{5\beta^8}\lambda^4(1-4\lambda+4\lambda^2)\right)IF_{D2}^2. \tag{28}$$

In Eqs. (26), (27), and (28) F_{D2} is defined by

$$F_{D2}=\frac{\beta^6}{\beta_A^{7/2}\beta_B^{5/2}}\exp\left(-\frac{p^2}{8(\beta_A^2+\beta_B^2)}\right). \tag{29}$$

V. RESULTS

We first give the numerical results for all relevant radiative decays. Discussion of these results is in two parts. The first treats decays to ^3P_J states, with the emphasis on unique signatures for specific vector $q\bar{q}$ states. The second deals with radiative decays to scalars as a flavor filter with implications for the scalar glueball mass. We then discuss qualitatively hybrid meson radiative transitions.

A. Numerical results

A simple test of the validity of Tables I and II is provided by the well-known decays $\rho\to\eta\gamma$, $\omega\to\eta\gamma$, $\phi\to\eta\gamma$, and $\phi\to\eta'\gamma$. The calculated widths in keV, using $\beta=0.313$ from Table I for the $n\bar{n}$ decays and $\beta=0.355$ from Table II for the $s\bar{s}$ decays but the physical masses in each case, are

TABLE III. Radiative widths for $1\ ^3S_1$ decays to $1\ ^1S_0$.

Decay	Model	Experiment
$\rho \to \eta\gamma$	39.6	36 ± 13
$\omega \to \eta\gamma$	4.7	5.5 ± 0.9
$\phi \to \eta\gamma$	92.7	57.82 ± 1.53
$\phi \to \eta'\gamma$	0.35	0.30 ± 0.15

compared with the experimental widths [1] in Table III. The agreement for the ρ and ω decays is clearly satisfactory; that for the decay $\phi \to \eta\gamma$ less so.

We can use the decays $\rho \to \pi\gamma$ and $\omega \to \pi\gamma$, again with physical masses, to estimate the appropriate value of β_π for decays to $\pi\gamma$. The variation of the width for $\omega \to \pi\gamma$ with β_π is shown in Fig. 1. At no point does it reach the experimental value [1] of 717 ± 43 keV. The maximum of the curve is 520 keV and occurs at $\beta_\pi = 0.335$, which we take to be the optimum value. The discrepancy between the model calculation and the experimental value is an indication of the uncertainty in the evaluation of decays to $\pi\gamma$.

The radiative decay widths for the $n\bar{n}$ states are given in Table IV. For purposes of illustration, we have assumed that the $f_0(1370)$ is a pure $n\bar{n}$ state and have ignored possible mixing in the 1^3P_0 nonet. This is certainly an oversimplification as there is good evidence [35], discussed in Sec. II, for scalar mixing within this nonet and with a scalar glueball. We return to this question below. The effect of phase space is clearly seen in the deviations from the naive 9:1 ratios of Eqs. (7) and (8). The radiative decay widths for the $s\bar{s}$ states are given in Table V. As for the $n\bar{n}$ decays, we have ignored mixing and assumed that the $f_0(1710)$ is pure $s\bar{s}$.

We have commented above on the uncertainties in the decays $\rho \to \pi\gamma$ and $\omega \to \pi\gamma$. The situation becomes even more uncertain for the decays $\rho(1450) \to \pi\gamma$ and $\omega(1420) \to \pi\gamma$. These decays proceed essentially via the spin-flip part of the amplitude which vanishes in the nonrelativistic limit for orthogonal wave functions. For Gaussian wave functions the amplitude is proportional to $(\beta^2/\beta_A^2 - 1) + 2\lambda^2 p^2/(3\beta_A^2)$ [see Eq. (14)] where the term $(\beta^2/\beta_A^2 - 1)$ measures the nonorthogonality of the wave functions. Note

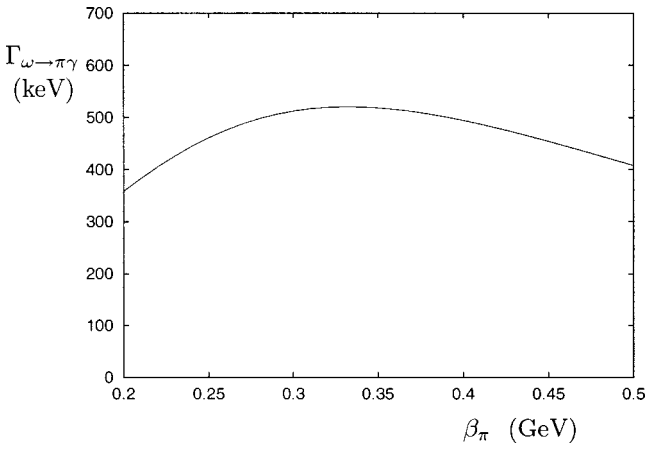

FIG. 1. Variation of the width for the decay $\omega \to \pi\gamma$ as a function of β_π with β_ω fixed at 0.313 according to Table I.

that one should not expect the radial wave functions of the 2^3S_1 and 1^1S_0 states to be orthogonal in the fully relativistic theory, as spin-dependent forces are not treated as perturbations there. With $\beta_A \neq \beta_B$ the resulting width is rather sensitive to the actual value of β_B. The value of β_π is not determined by the model, and as the width for $\omega \to \pi\gamma$ varies rather slowly with β_π, our choice of $\beta_\pi = 0.335$ has a rather large error. The effect on the width of $\omega(1420) \to \pi\gamma$ of varying β_π is shown in Fig. 2.

The first term in Eq. (14) increases rapidly with increasing β_π, and for β_π in the range we are considering it is this term and the interference term that dominate the width. The direct contribution from the second term in Eq. (14) becomes increasingly unimportant. A similar result holds for the decays $\rho(1450) \to \eta\gamma$ and $\omega(1429) \to \eta\gamma$ as can be seen in Fig. 3. As a consequence we suggest that the errors on the $2S$ decays to $\pi\gamma$ and $\eta\gamma$ are of the order of $\pm 50\%$.

An estimate of the uncertainties for other decays can be obtained by looking at the contributions from terms in increasing powers n of p^2/β^2. These are given in Table VI, as percentages, for some of the larger widths.

The implications of Table VI are that the results for the decays of $\rho(1450)$ to $f_1(1285)\gamma$ and $f_2(1270)\gamma$ and the corresponding $\omega(1420)$ decays to $a_1(1260)\gamma$ and $a_2(1320)\gamma$ are

TABLE IV. Results for radiative decays of $n\bar{n}$ states in keV.

	$\Gamma(\rho(1450))$	$\Gamma(\omega(1420))$	$\Gamma(\rho(1700))$	$\Gamma(\omega(1650))$
$\pi\gamma$	61	510	3.8	40
$\eta\gamma$	106	11	12	1.1
$\eta'\gamma$	61	5.7	6	0.5
$\pi(1300)\gamma$	5.9	29	0.4	1.7
$\eta(1295)\gamma$	57	3.6	3.9	0.2
$f_0(1370)\gamma$	64	4.7	899	88
$a_0(1450)\gamma$			82	612
$f_1(1285)\gamma$	349	33	1097	106
$a_1(1260)\gamma$	43	341	129	1016
$f_2(1270)\gamma$	712	67	148	13
$a_2(1320)\gamma$	59	413	13	91

TABLE V. Results for radiative decays of $s\bar{s}$ states in keV.

	$\Gamma(\phi(1680))$	$\Gamma(\phi(1930))$
$\eta\gamma$	94	9
$\eta'\gamma$	21	1.8
$\eta(1440)\gamma$	47	10
$f_0(1710)\gamma$		188
$f_1(1420)\gamma$	148	408
$f_2(1525)\gamma$	199	37

very reliable, the decay of $\rho(1700)$ to $f_0(1370)\gamma$ is solid, but the decay of $\rho(1700)$ to $f_1(1285)\gamma$ and the corresponding $\omega(1650)$ decay to $a_1(1260)\gamma$ should be treated with caution. This is not suprising because of the considerable increase in phase space. The situation is similar for the decays of $\phi(1690)$ and $\phi(1900)$, with the $f_1(1420)\gamma$ decay of the latter being the only one with any degree of uncertainty.

B. Decays to ^3P_J states

It is clear from Table IV that some decays provide very clear signatures for particular excitations. Obvious ones are $\rho(1450)\to f_2\gamma$ and $\omega(1420)\to a_2\gamma$; $\rho(1700)\to f_0\gamma$ and $\omega(1650)\to a_0\gamma$; $\rho(1700)\to f_1\gamma$ and $\omega(1650)\to a_1\gamma$. However, in e^+e^- annihilation experiments, isovector states are produced at approximately nine times the rate of the corresponding isoscalar states. Thus, for example, the effective $a_0\gamma$ rate from the decay of $\omega(1650)$ will be the same as that from $\rho(1700)$. Conversely, the contamination of the $f_2\gamma$ decay of $\rho(1450)$ by the corresponding decay of $\omega(1420)$ will only be at the 1% level. The $f_2(1525)\gamma$ decay of the $\phi(1690)$ is important as it provides a unique signature for the $s\bar{s}$ state, since in contrast to hadronic decays it is unaffected by $\omega(1650)$ and $\phi(1690)$ mixing. As we argue in Sec. V D radiative decays of a hybrid ρ_H to $f_2\gamma$ and of a hybrid ϕ_H to $f_2(1525)\gamma$ are strongly suppressed, so there is no ambiguity.

Although the $f_1(1420)\gamma$ decay of the $\phi(1900)$ looks like a clean signature of this state, it should be recalled that the value quoted in Table V should be treated with some caution. Despite this uncertainty, the width is necessarily much larger than that for the $\eta(1440)\gamma$ decay. This provides a mechanism for producing the $f_1(1420)$ without contamination from $\eta(1440)$ with which it shares many common hadronic decay channels.

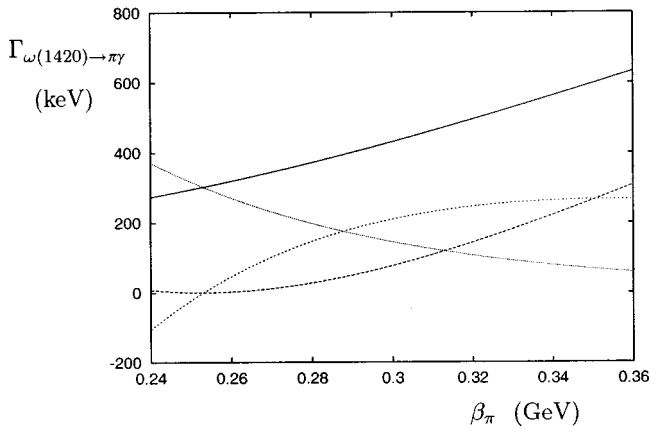

FIG. 2. Variation of the width for the decay $\omega(1420)\to\pi\gamma$ as a function of β_π. The solid line is the total width, the dashed line is the contribution from the first term in Eq. (14), the dotted line is the contribution from the second term in Eq. (14), and the short-dashed line is the contribution from the interference term.

It should be noted that there is some uncertainty about the mass of the $\rho(1450)$ and $\omega(1420)$. For the isovector states, the most extreme low mass comes from an analysis of the $\pi^+\pi^-$ spectrum in the reaction $K^-p\to\pi^+\pi^-\Lambda$ [43], which gives 1266 ± 14 MeV. An equally low mass, 1250 ± 29 MeV, has been suggested [44] for the isoscalar channel from an analysis of $e^+e^-\to\pi^+\pi^-\pi^0$. Given this uncertainty, we show the mass variation of the width for the decay of the isovector radial (2^3S_1) excitation to $f_2\gamma$ in Fig. 4.

C. Scalar mesons and glueballs

In Tables IV and V we assumed that there is no mixing among the scalars, so that the $f_0(1370)$ is pure $n\bar{n}$ and the $f_0(1710)$ is pure $s\bar{s}$. The result of the mixing is that the bare $n\bar{n}$ and $s\bar{s}$ states contribute in varying degrees to each of the $f_0(1370)$, $f_0(1500)$, and $f_0(1710)$. The variations of the radiative decay width of the $\rho(1700)$ and $\phi(1900)$ as functions of the mass of the f_0 are shown in Figs. 5 and 6, respectively.

Three different mixing scenarios have been proposed: the bare glueball is lighter than the bare $n\bar{n}$ state (the light glueball solution); the mass of the bare glueball is between the bare $n\bar{n}$ state and the bare $s\bar{s}$ state (the middleweight glueball solution); and the mass of the bare glueball is greater than the mass of the bare $s\bar{s}$ state. The first two solutions

TABLE VI. Contributions, in percent, from terms in increasing powers n of p^2/β^2.

	$n=0$	$n=1$	$n=2$	$n=3$	$n=4$
$\rho(1450)\to f_1(1285)\gamma$	106.2	−6.4	0.2		
$\rho(1450)\to f_2(1270)\gamma$	93.1	6.6	0.3		
$\rho(1700)\to f_0(1370)\gamma$	85.4	14.8	−0.2	−0.1	0.1
$\rho(1700)\to f_1(1285)\gamma$	56.5	39.6	4.7	−0.9	0.1
$\phi(1680)\to f_1(1420)\gamma$	112.7	−13.5	0.8		
$\phi(1680)\to f_2(1525)\gamma$	95.0	4.8	0.2		
$\phi(1900)\to f_0(1710)\gamma$	94.7	5.3	0.0	0.0	0.0
$\phi(1900)\to f_1(1420)\gamma$	52.1	43.2	6.0	−1.4	0.1

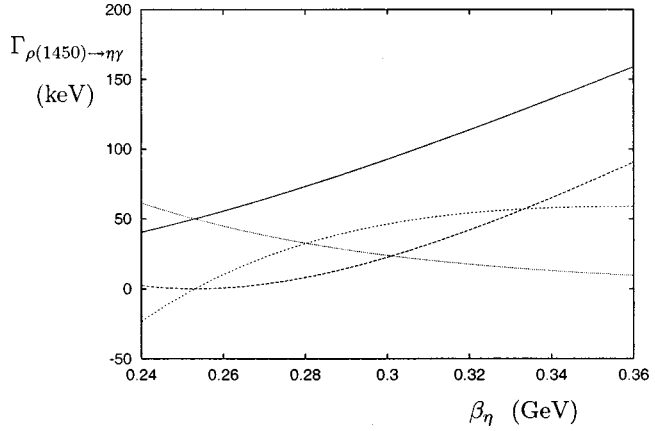

FIG. 3. Variation of the width for the decay $\rho(1450)\to\eta\gamma$ as a function of β_η. The solid line is the total width, the dashed line is the contribution from the first term in Eq. (14), the dotted line is the contribution from the second term in Eq. (14), and the short-dashed line is the contribution from the interference term.

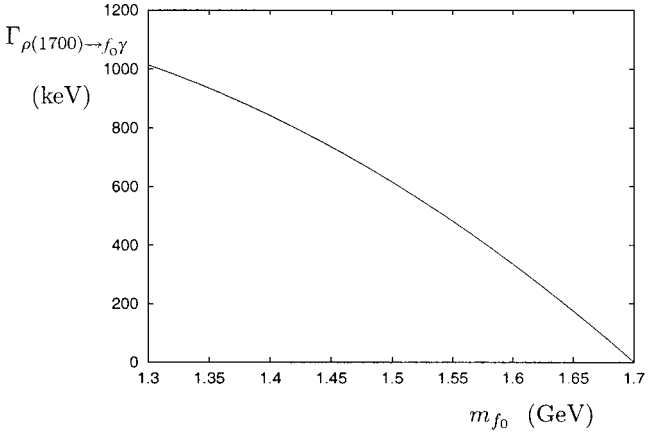

FIG. 5. Variation of the width for the decay $\rho(1700)\to f_0\gamma$ as a function of the mass of the f_0.

have been obtained in [35] and the third has been suggested in [34]. The effects of the mixing on the radiative decay widths of the $\rho(1700)$ and the $\phi(1900)$ to the three f_0 states are given in Table VII for each of these three cases.

The relative rates of the radiative decays of the $\rho(1700)$ to $f_0(1370)$ and $f_0(1500)$ change radically according to the presence of the glueball admixture. So for a light glueball the decay to $f_0(1370)$ is relatively suppressed whereas for a heavy glueball it is substantial. By contrast the effect on the decay to $f_0(1500)$ goes the other way. Further, the $\phi(1900)$ would give a large width for the decay to $f_0(1500)$ for a heavy glueball, but essentially zero for a light one. The $f_0(1710)$ will be prominent in the decays of the $\phi(1900)$ for all but the heaviest glueball. It is clear that these decays do provide an effective flavor-filtering mechanism.

Further, identifying the appropriate mixing scheme gives insight into the underlying physics of glueballs. The existing phenomenology from hadronic decays seems to favor a light glueball. Essentially, if the decays of the ''bare'' glueball are flavor independent, then the observed flavor dependencies for the hadronic decays of the physical mesons require [35] the glueball mass to be at the low end of the range preferred by quenched-lattice studies.

The resolution of the isoscalar-scalar problem is intimately connected with the isovector-scalar problem. The existence of any a_0 other than the $a_0(980)$ remains controversial. The different mixing schemes for the isoscalar-scalar mesons give rather different values for the mass of the bare $n\bar{n}$ state. This mass will be reflected in the mass of its isovector partner, the a_0. We see from Table IV that the width for the decay $\omega(1650)\to a_0\gamma$ is large, and from Table VI that it is a well-defined decay. So this decay can provide independent information on the existence and properties of the $a_0(1450)$.

D. Hybrid meson radiative transitions

Radiative transitions between hybrid states in the mass range under consideration are essentially ones in which spin flip is required. As the $q\bar{q}$ pair is in a spin-singlet state for a 1^{--} hybrid and in a spin-triplet state for 0^{-+}, 1^{-+}, and 2^{-+} hybrids, then, analogously to Eq. (13), for the transition $(1^{--})_H\to(J^{-+})_H\gamma$ one has

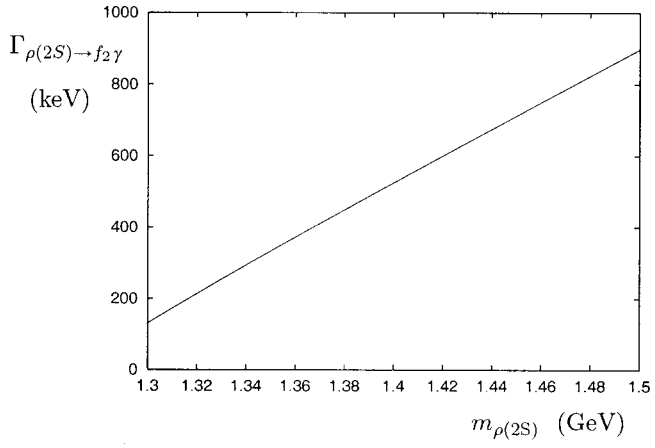

FIG. 4. Variation of the width for the decay $\rho(2S)\to f_2\gamma$ as a function of the mass of the $\rho(2S)$.

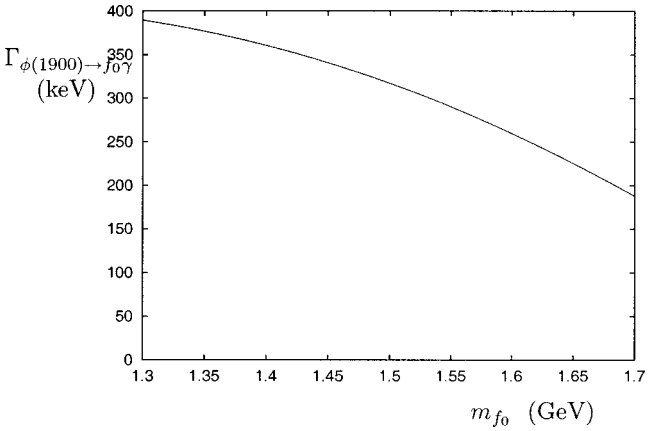

FIG. 6. Variation of the width for the decay $\phi(1900)\to f_0\gamma$ as a function of the mass of the f_0.

TABLE VII. Effect of mixing in the scalar sector of the 1^3P_0 nonet. The radiative widths, in keV, are given for three different mixing scenarios as described in the text: light glueball (*L*), middle-weight glueball (*M*), and heavy glueball (*H*).

	$\rho(1700)$			$\phi(1900)$		
	L	*M*	*H*	*L*	*M*	*H*
$f_0(1370)$	174	440	603	7	8	31
$f_0(1500)$	520	301	98	5	35	261
$f_0(1710)$				173	156	17

$$\Gamma = \frac{2J+1}{3}\frac{4}{3}\alpha p \frac{E_B}{m_A}\frac{p^2}{m_q^2} I F_H^2 \tag{30}$$

where F_H is a form factor similar to Eq. (16), unknown but of the order of unity. If the mass ordering is indeed $0^{-+} < 1^{-+} < 1^{--} < 2^{-+}$, the radiative decays of hybrid vectors to hybrid pseudoscalars and to exotic hybrids should be present but with widths less than 50 keV, the exact value depending on the phase space. However, if the mass ordering is the reverse, then the transition $(0^{-+})_H \to (1^{--})_H \gamma$ is possible. With $J=1$ in Eq. (30), then for the decay $\pi_H(1800) \to \omega_H(1500)$ this gives a rather healthy width of about 300 keV. Thus the decay $\pi(1800) \to \omega(1420)$ or $\omega(1650)$ is a potential discriminator among various assignments for both $\pi(1800)$ and the two ω states. For example, if the $\pi(1800)$ is a 3^1S_0 $q\bar{q}$ state, these radiative decays will be very strongly suppressed, with a width $\leqslant 1$ keV because of the orthogonality of the wave functions, unless the $\omega(1420)$ or $\omega(1650)$ is 3^3S_1, which is highly unlikely. Equally, if the $\pi(1800)$ is a 2^1S_0 $q\bar{q}$ state, then these radiative decays will have a width of more than 1000 keV. Thus if a radiative width of several hundred keV is found, then the two states must be siblings, which should be most natural for hybrids.

So we note a clear hierarchy. The radiative decay width is $O(1\,\text{MeV})$ for $q\bar{q}$ states in the same spatial state ($2S$ to $2S$ or $3S$ to $3S$); it is $O(300\,\text{keV})$ for hybrid to hybrid; and it is $O(1\,\text{keV})$ for $3S$ to $2S$. Heuristically, the $2S$ to $2S$ is big because of phase space, the hybrid likewise but reduced by the gluon-quark spin coupling while the $3S$ to $2S$ is destroyed by the orthogonality of the wave functions.

Radiative transitions between hybrids and $q\bar{q}$ mesons are the most uncertain. In constituent gluon models such transitions are highly suppressed as it is necessary to remove the gluon and to rearrange the color degrees of freedom. In the flux-tube model the mechanism is less explicit, and it has been argued [45] that the flux tube is excited as readily as a quark, with no extra suppression for radiative transitions between hybrids and $q\bar{q}$ states. However, even with no such suppression, the radiative decay of hybrid vectors to ${}^3P_J$ $q\bar{q}$ states is small as the transition is necessarily magnetic spin flip and is also suppressed by the phase space. This contrasts with the radiative decay of $q\bar{q}$ vector mesons to ${}^3P_J$ $q\bar{q}$ mesons, which proceeds in leading order by an electric transition. We shall report on this issue elsewhere.

VI. CONCLUSIONS

In Table VIII we show the final states for the dominant decays listed in Tables IV and V. Obviously, the experimentally cleanest signals come from the $\pi^+\pi^-$ decay of $f_2(1270)$ in $\rho^0(1450) \to f_2(1270)\gamma$ and the K^+K^- decay of $f_2(1525)$ in $\phi(1690) \to f_2(1525)\gamma$. The advantages are that the final-state mesons are comparatively narrow, their decays are two body, and there are no neutrals in the final state other than the photon. Additionally, these are decays for which the calculation is well defined and the answers reliable, as we discussed in relation to Table VI. An experimental check on the validity of the quark-model approach, apart from the total rate, is provided by the decay angular distribution. From Table VI and Eq. (A6) we see that we expect the electric-dipole term to dominate and to give a nearly isotropic angular distribution $d\Gamma/d\cos\theta \propto 1+\cos^2\theta/13$. Any significant deviation from this would imply an unexpectedly strong contribution from the magnetic-dipole term. These two decays are unique identifiers of the $\rho(1450)$ and the $\phi(1690)$, respectively. As discussed in the previous section, radiative decays of a hybrid ρ_H or ϕ_H to these final states are strongly suppressed and so there is no ambiguity.

The decay $\phi(1900) \to f_1(1420)\gamma$ discriminates between the $f_1(1420)$ and the $\eta(1440)$, as can be seen from Table V. The nearness of the masses and widths of these two states, and several common hadronic decay modes, have hitherto been sources of confusion. Although the magnitudes of the calculated radiative decays of the 1^3D_1 states are subject to some uncertainty, the width of $\phi(1900) \to f_1(1420)\gamma$ is necessarily much larger than that of $\phi(1900) \to \eta(1440)\gamma$. In the latter case the overlap of the wave functions leads to a much stronger suppression of the decay than in the former case, in any model.

The relative rates of the radiative decays of the $\rho(1700)$ to $f_0(1370)$ and $f_0(1500)$, and of the $\phi(1900)$ to $f_0(1500)$ and $f_0(1710)$, change radically according to the particular model for $q\bar{q}$-glueball mixing. The differences are sufficiently great, as can be seen in Table VII, for the appropriate mixing scheme to be identified and the glueball mass determined. The physics that can be extracted from these decays is significant and merits every effort to overcome the experimental problem posed by the multiplicity of hadronic decay channels of the scalars.

TABLE VIII. Final states for the dominant radiative decays of Tables IV and V.

Decay	Final state
$\rho^0(1450) \to f_1(1285)\gamma$	$4\pi\gamma, \eta\pi\pi\gamma$
$\rho^0(1450) \to f_2(1270)\gamma$	$\pi\pi\gamma$
$\omega(1420) \to a_1(1260)\gamma$	$\pi^+\pi^-\pi^0\gamma$
$\omega(1420) \to a_2(1260)\gamma$	$\pi^+\pi^-\pi^0\gamma$
$\phi(1680) \to f_1(1420)\gamma$	$K\bar{K}\pi\gamma$
$\phi(1680) \to f_2(1525)\gamma$	$K\bar{K}\gamma$
$\phi(1900) \to f_1(1420)\gamma$	$K\bar{K}\pi\phi$

The observation of the decay $\omega(1650)\to a_0(1450)\gamma$ is of high priority as it establishes consistency between the masses of the isoscalar and isovector $n\bar{n}$ states, with implications for the scalar glueball mass. Fortunately, the $a_0(1450)$ has comparatively simple decay modes, such as $K\bar{K}$.

The larger partial widths should be measurable at the new high-intensity facilities being proposed. In some cases they may be measurable in the data from present experiments. We give two specific examples. The $\omega\eta$ decay of the $\omega(1650)$ has been observed in the E852 experiment [46]. If the $\omega(1650)$ is the $1D$ $q\bar{q}$ excitation of the ω, then the $^3P_0$ model gives the partial width for this decay as 13 MeV [6]. The partial width for the radiative decay $\omega(1650)\to a_1(1260)\gamma$ is of the order of 1 MeV, that is, about 8% of the $\omega\eta$ width. The E852 experiment has several thousand events in the $\omega\eta$ channel, so we may expect several hundred events in the $a_1\gamma$ channel. Similarly, both the $\rho(1450)$ and $\rho(1700)$ are seen by the VES Collaboration [47] in the $\rho\eta$ channel with several thousand events. Both these states have strong radiative decays, the $\rho(1450)$ to $f_2(1270)\gamma$ and the $\rho(1700)$ to $f_1(1285)\gamma$. Assuming that the $\rho(1450)$ and $\rho(1700)$ are, respectively, the $2S$ and $1D$ excitations of the ρ, then the $^3P_0$ model gives the partial widths for the $\rho\eta$ decays of the $\rho(1450)$ and $\rho(1700)$ as 23 and 25 MeV, respectively, so the radiative decays could again be present at the level of a few hundred events.

ACKNOWLEDGMENTS

This work was supported, in part, by grants from the Particle Physics and Astronomy Research Council, RFBR 00-15-96786, INTAS-RFBR 97-232, and the European Community Human Mobility Program Eurodafne NCT98-0169.

APPENDIX A: ANGULAR DISTRIBUTIONS

In the following equations the isospin factors I are given in Eqs. (7) and (8), λ in Eq. (12), and β in Eq. (11). The form factors F_{S1}, F_{S2}, F_{D1}, and F_{D2} are defined in Eqs. (16), (20), (25), and (29) and the functions G_E and G_M in Eqs. (21) and (22):

$1^3S_1\to1^1S_0$

$$\frac{d\Gamma_S^0}{d\cos\theta}=\frac{1}{2}\alpha p\frac{E_B}{m_A}\frac{p^2}{m_q^2}(1+\cos^2\theta)IF_{S1}^2. \tag{A1}$$

$2^3S_1\to1^1S_0$

$$\frac{d\Gamma}{d\cos\theta}=\frac{3}{2}\left[\left(\frac{\beta^2}{\beta_A^2}-1\right)+\frac{2\lambda^2p^2}{3\beta_A^2}\right]^2\frac{d\Gamma_S^0}{d\cos\theta}. \tag{A2}$$

$2^3S_1\to2^1S_0$

$$\frac{d\Gamma}{d\cos\theta}=\frac{9}{4}\left[\left(\frac{5\beta^4}{3\beta_A^2\beta_B^2}-1\right)+\frac{4\lambda^2p^2}{3\beta^2}\left(\frac{\beta^4}{3\beta_A^2\beta_B^2}-1\right)+\frac{4\lambda^2p^4}{9\beta_A^2\beta_B^2}\right]^2\frac{d\Gamma_S^0}{d\cos\theta}. \tag{A3}$$

$2^3S_1\to1^3P_0$

$$\frac{d\Gamma}{d\cos\theta}=\frac{2}{9}\alpha p\frac{E_B}{m_A}\frac{\beta^2}{m_q^2}(1+\cos^2\theta)\left(1-\frac{p^2}{2\beta^2}\right)\times\left[G_E^2-\frac{p^2}{2\beta^2}G_EG_M+\frac{1}{16}\left(\frac{p^2}{\beta^2}\right)^2G_M^2\right]IF_{S2}^2. \tag{A4}$$

$2^3S_1\to1^3P_1$

$$\frac{d\Gamma}{d\cos\theta}=\alpha p\frac{E_B}{m_A}\frac{\beta^2}{m_q^2}\left[(1-\tfrac{1}{3}\cos^2\theta)G_E^2-\frac{p^2}{3\beta^2}(1-\cos^2\theta)G_EG_M+\frac{1}{24}\left(\frac{p^2}{\beta^2}\right)^2(1-\cos^2\theta)G_M^2\right]IF_{2S}^2. \tag{A5}$$

$2^3S_1\to1^3P_2$

$$\frac{d\Gamma}{d\cos\theta}=\frac{13}{9}\alpha p\frac{E_B}{m_A}\frac{\beta^2}{m_q^2}\left[(1+\tfrac{1}{13}\cos^2\theta)G_E^2+\frac{2p^2}{13\beta^2}(2-\cos^2\theta)G_EG_M+\frac{1}{104}\left(\frac{p^2}{\beta^2}\right)^2(5-3\cos^2\theta)G_M^2\right]IF_{2S}^2. \tag{A6}$$

$1^3D_1\to1^1S_0$

$$\frac{d\Gamma_D^0}{d\cos\theta}=\frac{1}{15}\alpha p\frac{E_B}{m_A}\lambda^4\frac{p^4}{\beta^4}\frac{p^2}{m_q^2}(1+\cos^2\theta)IF_{D1}^2. \tag{A7}$$

$1^3D_1\to2^1S_0$

$$\frac{d\Gamma}{d\cos\theta}=\frac{3}{2}\left[\left(\frac{2\lambda^2p^2}{3\beta_B^2}-1\right)+\frac{7\beta^2}{3\beta_B^2}\right]^2\frac{d\Gamma_D^0}{d\cos\theta}. \tag{A8}$$

$1^3D_1 \to 1^3P_0$

$$\frac{d\Gamma}{d\cos\theta} = \frac{10}{9}\alpha p \frac{E_B}{m_A}\frac{\beta^2}{m_q^2}(1+\cos^2\theta)\left(1+\frac{p^2}{5\beta^2}\lambda(1+2\lambda)+\frac{p^4}{5\beta^4}\lambda^2(-1+2\lambda)\right)^2 IF_{D2}^2. \tag{A9}$$

$1^3D_1 \to 1^3P_1$

$$\begin{aligned}\frac{d\Gamma}{d\cos\theta} = \frac{5}{6}\alpha p \frac{E_B}{m_A}\frac{\beta^2}{m_q^2}\Bigg(&\frac{1}{2}(3-\cos^2\theta)+\frac{p^2}{5\beta^2}\lambda[11-5\cos^2\theta+2\lambda(3-\cos^2\theta)]\\&+\frac{p^4}{50\beta^4}\lambda^2[1+17\cos^2\theta+4\lambda(31-25\cos^2\theta)+4\lambda^2(3-\cos^2\theta)]\\&+\frac{8p^6}{25\beta^6}\lambda^3(1-\cos^2\theta)(-2+3\lambda+2\lambda^2)\\&+\frac{4p^8}{25\beta^8}\lambda^4(1-\cos^2\theta)(1-4\lambda+4\lambda^2)\Bigg)IF_{D2}^2.\end{aligned} \tag{A10}$$

$1^3D_1 \to 1^3P_2$

$$\begin{aligned}\frac{d\Gamma}{d\cos\theta} = \frac{1}{15}\alpha p \frac{E_B}{m_A}\frac{\beta^2}{m_q^2}\Bigg(&\frac{1}{12}(13+\cos^2\theta)\\&+\frac{p^2}{6\beta^2}\lambda(11+35\cos^2\theta)+2\lambda(17-43\cos^2\theta)\\&+\frac{p^4}{12\beta^4}\lambda[83(1+\cos^2\theta)-4\lambda(103+7\cos^2\theta)+20\lambda^2(41-19\cos^2\theta)]\\&+\frac{p^6}{3\beta^6}\lambda^3(17-7\cos^2\theta)-12\lambda(9-5\cos^2\theta)+4\lambda^2(37-23\cos^2\theta)\\&+\frac{p^8}{3\beta^8}\lambda^4(7-5\cos^2\theta)(1-4\lambda+4\lambda^2)\Bigg)IF_{D2}^2.\end{aligned} \tag{A11}$$

APPENDIX B: RADIATIVE HELICITY AMPLITUDES

In this appendix we show how the amplitudes used in the main body of this paper are related to helicity amplitudes that appear elsewhere in the literature. This also enables application of some of our results, which have been specified for e^+e^- annihilation, to be taken over to photoproduction.

Following [48,49] the electromagnetic interaction may be written in the form

$$J_{\text{e.m.}} = \sum_{j=1}^{2} e_j \mu(-2i\vec{s}\cdot\vec{p}\times\vec{A} - g^{-1}(\vec{k}+\vec{k}')\cdot\vec{A}), \tag{B1}$$

where e_j is the quark charge in units of e, $\mu \equiv g\sqrt{\alpha/2m_q} = 0.13\ \text{GeV}$ is the quark-scaled magnetic moment, and $\vec{A} = \vec{\epsilon}\sqrt{4\pi/2\omega}e^{i\vec{p}\cdot\vec{r}_j}$. Choosing the $\hat{z}$ axis to be along the photon momentum, and $\vec{\epsilon} = -(1/\sqrt{2})(1,i,0)$ for $J_z = +1$ then Eq. (B1) becomes

$$J_{\text{e.m.}} = 2\sqrt{\pi/\omega}\mu\sum_{j=1}^{2} e_j[p(S_x+iS_y) + g^{-1}(k_x+ik_y)]e^{ipz} \tag{B2}$$

to be compared with Eq. (7.3) in [49], whereby after summing over two quarks the matrix element becomes

$$4\sqrt{\pi/\omega}\mu\langle e\rangle(p\langle\sigma_+\rangle R_{L0} + g^{-1}\langle L_+\rangle R_{L1}) \tag{B3}$$

where $\langle e\rangle^2 \equiv I$ of Eq. (6) and

$$R_{L1} \equiv \left\langle \psi_{L1}^* \middle| e^{ipr/2}(-i)\frac{d}{dr}\middle| \psi_{00}\right\rangle,$$

$$R_{L0} \equiv \langle \psi_{L0}^* | e^{ipr/2} | \psi_{00}\rangle, \tag{B4}$$

where the ψ_{L,L_z} are the bound-state wave functions for the $q\bar{q}$ state with orbital angular momentum L,L_z [48].

Radiative widths are then

$$\frac{\Gamma(A\to B\gamma)}{8m_A E_B}=\frac{p}{8\pi m_A^2}\frac{2J_B+1}{2J_A+1}\langle e\rangle^2\sum_\lambda |M_\lambda|^2 \qquad \text{(B5)}$$

and $\omega\equiv|p|$ for real photons; $\langle e\rangle=\frac{1}{2}$ for $I=0\to I=1$, $\langle e\rangle=\frac{1}{6}$ for $I=0$ $(1)\to I=0$ (1), and the M_λ are helicity amplitudes with helicity λ.

1. $M1$ transitions

As an illustration and check on the normalization we compute $\Gamma(\omega\to\pi\gamma)$.

The matrix element becomes ($\langle\sigma_+\rangle=1/\sqrt{2}$)

$$M_{+1}=\mu\sqrt{2\pi p}R_{L0} \qquad \text{(B6)}$$

for $J_z^\gamma=+1$ and $\langle e\rangle=1/2$. Hence

$$\Gamma(\omega\to\pi\gamma)=\frac{4}{3}\mu^2p^3\frac{E_\pi}{m_\omega}|R_{00}(p)|^2$$
$$\to\frac{4}{3}\alpha p\frac{E_\pi}{m_\omega}\frac{gp^2}{m_q^2}\frac{1}{4}|R_{00}(p)|^2, \qquad \text{(B7)}$$

to be compared with Eq. (13) with $m_q=0.33$, $g=1$. In the harmonic oscillator basis

$$R_{00}(p)\equiv\exp\left(-\frac{p^2}{16\beta^2}\right) \qquad \text{(B8)}$$

which is the $\beta_A=\beta_B$ limit of F_{S1} of Eq. (16). Hence if $\beta\sim0.4$ GeV [4–6], then

$$\Gamma(\omega\to\pi\gamma)\sim0.6\ \text{MeV}. \qquad \text{(B9)}$$

In the text we show that this value for β does not fit well with the detailed spectroscopy, and when realistic values are used, the actual width for $\omega\to\pi\gamma$ is somewhat reduced (see Fig. 1).

An analogous calculation for the radiative transition from the $\omega(2^3S_1)$ involves a radial wave function and different magnitude for p,p^* say. Thus

$$\frac{\Gamma(\omega(2^3S_1)\to\pi\gamma)}{\Gamma(\omega\to\pi\gamma)}=\left(\frac{p^*}{p}\right)^3\frac{1}{6}\left(\frac{p^{*2}}{8\beta^2}\right)^2\exp\left(\frac{p^2-p^{*2}}{8\beta^2}\right). \qquad \text{(B10)}$$

This also sets the scale for transitions between $\pi(1800)$ and $\omega(1420/1650)$ which potentially bear on the question of hybrid states.

2. Application to excited states: $E1$ and $M2$ transitions

Helicity amplitudes follow from the most general form of the single quark interaction with a transversely polarized photon in the algebraic form [49]

$$J_+^{\text{e.m.}}=(AL_++B\sigma_++C\sigma_zL_++D\sigma_-L_{++})4\mu\sqrt{\pi p}\langle e\rangle. \qquad \text{(B11)}$$

In the nonrelativistic limit $C\equiv D=0$ and

$$A\langle L_+\rangle\equiv R_{L1}/pg,$$
$$B\langle\sigma_+\rangle\equiv R_{L0}/\sqrt{2}. \qquad \text{(B12)}$$

We will be particularly interested in transitions between $2S$ and $1P$ states. In the Gaussian wave function approach we have

$$A\langle L_+\rangle\equiv R_{L1}/pg$$
$$=\frac{i\beta\sqrt{2}}{pg\sqrt{3}}\left(1+\frac{p^2}{16\beta^2}\right)\exp\left(\frac{-p^2}{16\beta^2}\right)$$
$$\equiv\frac{i\beta\sqrt{2}}{gp\sqrt{3}}G_E,$$
$$B\langle\sigma_+\rangle\equiv R_{L0}/\sqrt{2}$$
$$=\frac{ip}{\beta2\sqrt{6}}\left(1-\frac{p^2}{16\beta^2}\right)\exp\left(\frac{-p^2}{16\beta^2}\right)$$
$$\equiv\frac{i\beta\sqrt{2}}{p\sqrt{3}}\left(\frac{p^2}{4\beta^2}\right)G_M. \qquad \text{(B13)}$$

If we are interested in terms only up to $O(p^4)$ we can approximate the above as

$$A(L_+)\to\frac{i\beta\sqrt{2}}{gp\sqrt{3}},$$
$$B(\sigma_+)\to\frac{ip}{\beta2\sqrt{6}}\left(1-\frac{p^2}{8\beta^2}\right). \qquad \text{(B14)}$$

The widths are then

$$\Gamma(\rho(2S)\to f_J\gamma)=(2J+1)\frac{8}{3}\left(\frac{\mu}{g}\right)^2p^3\frac{E_j}{m_\rho}\sum_{\lambda\geqslant0}|M_\lambda|^2, \qquad \text{(B15)}$$

where λ refers to the helicity of the state and the matrix elements $|M_\lambda|$ are

$$f_0: M_0=(A-B)/\sqrt{3}, \qquad \text{(B16)}$$
$$f_1: M_0=A/\sqrt{2},$$
$$M_1=(A-B)/\sqrt{2},$$
$$f_2: M_0=(A+2B)/\sqrt{6},$$
$$M_1=(A+B)/\sqrt{2},$$
$$M_2=A.$$

As a specific application,

$$\Gamma(\rho(2S)\to f_0\gamma)=\frac{8}{3}\left(\frac{\mu}{g}\right)^2 p^3\frac{E_{f0}}{m_\rho}|(A-B)/\sqrt{3}|^2$$
$$=\frac{4}{27}\frac{\alpha}{m_q^2}p\beta^2\frac{E_{f0}}{m_\rho}$$
$$\times\left[\left(1+\frac{p^2}{16\beta^2}\right)-g\frac{p^2}{4\beta^2}\right]^2\exp\left(-\frac{p^2}{8\beta^2}\right)$$
$$=\frac{4}{27}\frac{\alpha}{m_q^2}p\beta^2\frac{E_{f0}}{m_\rho}\left(G_E-\frac{p^2}{4\beta^2}G_M\right)^2F^2 \quad \text{(B17)}$$

using $\mu/g\equiv\sqrt{\alpha}/2m_q$. The form in Eq. (17) reduces to this in the particular case where all β values are the same and the isospin factor $I=1/4$.

Note also the following translations:

$$G_E\equiv\sqrt{\tfrac{3}{2}}\frac{p}{\beta}A,$$
$$G_M\equiv\sqrt{\tfrac{3}{2}}\frac{p}{\beta}\frac{p^2}{4\beta^2}B. \quad \text{(B18)}$$

[1] Particle Data Group, D. Groom *et al.*, Eur. Phys. J. C **15**, 1 (2000).
[2] S. Godfrey and N. Isgur, Phys. Rev. D **32**, 189 (1985).
[3] G. Busetto and L. Oliver, Z. Phys. C **20**, 247 (1983); P. Geiger and E. S. Swanson, Phys. Rev. D **50**, 6855 (1994); H. G. Blundell and S. Godfrey, *ibid.* **53**, 3700 (1996).
[4] R. Kokoski and N. Isgur, Phys. Rev. D **35**, 907 (1987).
[5] E. S. Ackleh, T. Barnes, and E. S. Swanson, Phys. Rev. D **54**, 6811 (1996).
[6] T. Barnes, F. E. Close, P. R. Page, and E. S. Swanson, Phys. Rev. D **55**, 4157 (1997).
[7] CMD Collaboration, R. R. Akhmetshin *et al.*, Phys. Lett. B **466**, 392 (1999).
[8] CLEO Collaboration, K. W. Edwards *et al.*, Phys. Rev. D **61**, 072003 (2000).
[9] A. Donnachie and Yu. S. Kalashnikova, Z. Phys. C **59**, 621 (1993).
[10] F. E. Close and P. R. Page, Phys. Rev. D **56**, 1584 (1997).
[11] A. Donnachie and Yu. S. Kalashnikova, Phys. Rev. D **60**, 114011 (1999).
[12] P. Lacock, C. Michael, P. Boyle, and P. Rowland, Phys. Lett. B **401**, 308 (1997).
[13] C. Bernard *et al.*, Phys. Rev. D **56**, 7039 (1997); C. McNeille *et al.*, Nucl. Phys. B (Proc. Suppl.) **73**, 264 (1999).
[14] P. Lacock and K. Schilling, Nucl. Phys. B (Proc. Suppl.) **73**, 261 (1999).
[15] C. McNeile, hep-lat/9904013.
[16] C. Morningstar, Nucl. Phys. B (Proc. Suppl.) **90**, 714 (2000).
[17] T. Barnes and F. E. Close, Phys. Lett. **116B**, 365 (1982); **123B**, 89 (1983); T. Barnes, F. E. Close, and F. de Viron, Nucl. Phys. **B224**, 241 (1983).
[18] M. Chanowitz and S. Sharpe, Nucl. Phys. **B222**, 211 (1983).
[19] N. Isgur and J. E. Paton, Phys. Lett. **124B**, 247 (1983); N. Isgur, R. Kokoski, and J. E. Paton, Phys. Rev. Lett. **54**, 869 (1985); N. Isgur and J. E. Paton, Phys. Rev. D **31**, 2910 (1985); T. Barnes, F. E. Close, and E. S. Swanson, *ibid.* **52**, 5242 (1995).
[20] Yu. S. Kalashnikova and Yu. B. Yufryakov, Phys. Lett. B **359**, 175 (1995); Phys. At. Nucl. **60**, 307 (1997).
[21] I. I. Balitsky, D. I. Dyakonov, and A. V. Yung, Z. Phys. C **33**, 265 (1986).
[22] J. I. Latorre, P. Pascual, and S. Narison, Z. Phys. C **34**, 347 (1987).
[23] E852 Collaboration, I. I. Ivanov *et al.*, Phys. Rev. Lett. **86**, 3977 (2001).
[24] E852 Collaboration, D. P. Weygand, in *HADRON'97*, edited by S.-U. Chung and H. J. Willutski (AIP, Woodbury, NY, 1998), p. 313.
[25] VES Collaboration, Yu. P. Gouz, in Proceedings of XXVI ICHEP, Dallas, 1992, edited by J. R. Sanford, p. 572.
[26] E852 Collaboration, D. R. Thompson *et al.*, Phys. Rev. Lett. **79**, 1630 (1997).
[27] Crystal Barrel Collaboration, A. Abele *et al.*, Phys. Lett. B **423**, 175 (1998).
[28] VES Collaboration, A. Zaitsev, in *HADRON'97* [24], p. 461; VES Collaboration, D. V. Amelin, *ibid.*, p. 770.
[29] UKQCD Collaboration, G. Bali *et al.*, Phys. Lett. B **309**, 378 (1993); Phys. Rev. D **62**, 054503 (2000); D. Weingarten, hep-lat/9608070; J. Sexton *et al.*, Phys. Rev. Lett. **75**, 4563 (1995); F. E. Close and M. Teper, Report No. RAL-96-040/OUTP-96-35; W. Lee and D. Weingarten, hep-lat/9805029; G. Bali, Phys. Rep. **343**, 1 (2001).
[30] C. Amsler and F. E. Close, Phys. Lett. B **353**, 385 (1995).
[31] F. E. Close, hep-ph/0110081.
[32] C. McNeile and C. Michael, Phys. Rev. D **63**, 114503 (2001).
[33] F. E. Close, G. R. Farrar, and Z. Li, Phys. Rev. D **55**, 5749 (1997).
[34] W. Lee and D. Weingarten, Phys. Rev. D **61**, 014015 (2000).
[35] F. E. Close and A. Kirk, Eur. Phys. J. C **21**, 531 (2001).
[36] WA102 Collaboration, D. Barberis *et al.*, Phys. Lett. B **479**, 59 (2000).
[37] Crystal Barrel Collaboration, C. Amsler *et al.*, Phys. Lett. B **333**, 277 (1994); **355**, 425 (1995); OBELIX Collaboration, A. Bertin *et al.*, *ibid.* **434**, 180 (1998).
[38] R. Bonnaz, B. Silvestre-Brac, and C. Gignoux, hep-ph/0101112.
[39] Yu. S. Kalashnikova, A. V. Nefediev, and Yu. A. Simonov, Phys. Rev. D **64**, 014037 (2001).
[40] A. P. Szczepaniak and E. S. Swanson, Phys. Rev. D **55**, 3987 (1997).
[41] F. J. Llanes-Estrada and S. R. Cotanch, Phys. Rev. Lett. **84**, 1102 (2000).

[42] A. P. Szczepaniak and E. S. Swanson, Phys. Rev. Lett. **87**, 072001 (2001).
[43] LASS Collaboration, D. Aston *et al.*, Nucl. Phys. B (Proc. Suppl.) **21**, 105 (1991).
[44] SND Collaboration, M. N. Achasov *et al.*, hep-ex/0109035.
[45] N. Isgur, Phys. Rev. D **60**, 114016 (1999).
[46] E852 Collaboration, P. Eugenio *et al.*, Phys. Lett. B **497**, 190 (2001).
[47] VES Collaboration, D. V. Amelin *et al.*, Nucl. Phys. **A668**, 83 (2000).
[48] L. A. Copley, G. Karl, and E. Obryk, Nucl. Phys. **B13**, 303 (1969); R. P. Feynman, M. Kislinger, and F. Ravndal, Phys. Rev. D **3**, 2706 (1971).
[49] F. E. Close, *Introduction to Quarks and Partons* (Academic, New York, 1978).